The selective oxidation of n-butane to maleic anhydride: comparison of bulk and supported V–P–O catalysts *

M. Ruitenbeek [a,**], A.J. van Dillen [a], A. Barbon [b], E.E. van Faassen [b], D.C. Koningsberger [a] and J.W. Geus [a]

[a] *Utrecht University, Debye Institute, Department of Inorganic Chemistry and Catalysis, PO Box 80.083, 3508 TB Utrecht, The Netherlands*
E-mail: m.ruitenbeek@chem.uu.nl

[b] *Utrecht University, Debye Institute, Section Interface Physics, PO Box 80.000, 3508 TA Utrecht, The Netherlands*

Received 10 June 1998; accepted 14 September 1998

V–P–O catalysts supported on the surface of silica and titania particles were studied and compared with bulk V–P–O. The catalytic performance was tested in the n-butane oxidation reaction to maleic anhydride, and the structure of the equilibrated catalysts was characterised with X-ray absorption spectroscopy (EXAFS) and (low-temperature) ESR spectroscopy. Our results show considerable differences in catalytic performance between VPO/TiO_2 on the one hand, and VPO/SiO_2 and VPO/bulk on the other hand, the yield to maleic anhydride being comparable for VPO/bulk and VPO/SiO_2. The differences in catalytic behaviour are attributed to differences in the local structure around vanadium (EXAFS). Furthermore, different spin exchange interactions between vanadium atoms in the three samples have been observed (ESR). The combination of characterisation methods suggests that the structure of the supported V–P–O phase is amorphous and differs considerably from that of bulk crystalline vanadylpyrophosphate. We therefore propose that the oxidation of n-butane to maleic anhydride takes place over an amorphous surface V–P–O phase. This finding has high relevance for our understanding of the catalytic activity of bulk crystalline V–P–O catalysts as well.

Keywords: supported V–P–O catalysts, silica, titania, vanadylpyrophosphate, butane oxidation, EXAFS, ESR spectroscopy, Curie–Weiss law, antiferromagnetic pairs

1. Introduction

Bulk catalysts based on vanadium–phosphorus–oxide (V–P–O) are industrially used for the production of maleic anhydride (MA) from n-butane. The V–P–O system has been under investigation for the last three decades, and although it is widely accepted that vanadylpyrophosphate, $(VO)_2P_2O_7$, is the main component in the active catalyst, still little is known about the exact nature of the catalytic active site [1–4].

At Utrecht University much effort is devoted to the development of supported V–P–O catalysts [5–7], as the supported V–P–O catalysts have superior characteristics over bulk V–P–O, such as a cheap and reproducible preparation procedure, a larger amount of active sites per unit surface area, a short activation period, and a high mechanical strength. Therefore, application of supported V–P–O catalysts in a fluidized-bed process is very promising.

The newly developed supported catalysts show interesting catalytic properties. For instance, titania-supported V–P–O is already active at moderate temperatures (523 vs. 673 K for the commercial bulk catalyst), although the selectivity is low [5,7]. Silica-supported V–P–O catalysts, on the other hand, show reasonable yields in maleic anhydride [6], and these systems are being further optimised in our laboratory.

In literature, only a few other examples of deposition of V–P–O on silica [8–10], titania [11], alumina [11–14] and $AlPO_4$ [15] have been described. Generally, the lack of long-range order of the supported V–P–O particles compromises a proper characterisation of the supported V–P–O phase with common techniques like X-ray diffraction or FTIR spectroscopy. Nevertheless, most supported V–P–O catalysts are reported to consist of a phase that strongly resembles V^{5+} phosphate, mostly γ-$VOPO_4$ or α-$VOPO_4$ [16,17].

Generally, the catalytic activity of the V–P–O catalysts has been related to the local structure of surface vanadyl groups in vanadylpyrophosphate. However, with most techniques, no explicit information about the active surface is obtained, since the data are obstructed by contributions of the bulk. The structure of crystalline vanadylpyrophosphate consists of pairs of edge-sharing pseudo-octahedrally coordinated vanadium ions at a distance of 3.23 Å, isolated from other pairs by pyrophosphate groups [18]. This structural unit is often used to model the active sites in V–P–O catalysts [2,19,20]. Moreover, in the literature, various other models have been proposed, i.e., interfaces between different $VOPO_4$ phases and $(VO)_2P_2O_7$ [16,17], V^{5+} sites on the surface of $(VO)_2P_2O_7$ [2], V^{5+} species in interaction with $VO(PO_3)_2$ [21], and amorphous V^{4+} and/or V^{5+} phases supported on crystalline $(VO)_2P_2O_7$ [22,23].

In this paper we describe our study on the structure–activity relationship of supported V–P–O catalysts. To this end we have applied X-ray absorption spectroscopy (EX-

* Netherlands Institute for Research in Catalysis (NIOK) publication # UU 98-1-05 and UU 98-2-02.

** To whom correspondence should be addressed.

AFS) and ESR spectroscopy. These techniques do not require crystallinity of the sample and provide information on the local microstructure around the vanadium site.

Our results support the view that the catalytic site of bulk V–P–O catalysts is an amorphous surface phase. Therefore, we are convinced that the local structure of our supported V–P–O phase resembles the structure of the amorphous surface of bulk V–P–O.

2. Experimental

2.1. Catalyst preparation

The catalysts used for this study were bulk V–P–O, titania-supported V–P–O (8.2 wt% V), and silica-supported V–P–O (7.5 wt% V). All catalysts were prepared with an atomic P/V ratio of 1.1. A bulk V–P–O catalyst was prepared in i-butanol according to a well-known procedure [24] and exhibited a crystalline structure [25].

Supported V–P–O catalysts have been prepared on TiO_2 (Degussa P25) and SiO_2 (Engelhard C500-20) according to a procedure described by Overbeek et al. [5,6]. In brief, the method comprises an electrochemical reduction of V^{5+} to V^{3+} ions in diluted hydrochloric acid solution, followed by homogeneous precipitation (HDP) of the V^{3+} species onto the supports in the presence of $NH_4H_2PO_4$. For the preparation of silica-supported catalysts, this method was slightly adapted, because of the poor interaction of the V–P–O with silica [6,26]. First an amount of vanadium precursor was precipitated in absence of a phosphate precursor. After drying at 393 K for 16 h, the supported vanadium oxide was subsequently impregnated with diluted phosphoric acid to obtain silica-supported V–P–O. The supported catalysts will be referred to as VPO/TiO_2 and VPO/SiO_2. The applied loadings compare to a calculated monolayer coverage of 2.0 and 2.7 for VPO/SiO_2 and VPO/TiO_2, respectively.

Catalyst precursors were calcined in N_2 at 723 K for 16 h prior to catalytic tests and subsequent characterisation.

2.2. Catalyst performance testing

After calcination, both bulk and supported V–P–O samples were tested in the selective oxidation of n-butane using a 1.5% n-butane, 20% O_2, 78.5% Ar flow (1.5 ml catalyst, 50 ml/min, GHSV = 2000 h^{-1}) at atmospheric pressure. Formed gaseous products as well as unconverted reactants were analysed using an on-line Balzers QMA-420 mass spectrometer operating at 150 °C to avoid condensation of products. Carbon mass balances were in the range of 0.98–1.02. A detailed description of the experimental conditions has been given in earlier publications [5,6].

2.3. Catalyst characterisation

All catalysts have been characterised with X-ray absorption spectroscopy (EXAFS) and ESR spectroscopy after equilibration in the butane oxidation reaction for more than 100 h.

EXAFS data were collected at Station 8.1 of the SRS facility in Daresbury (UK). The energy of the electron beam was 2 GeV (average current ∼150 mA). The Si [111] double-crystal monochromator was detuned to 70% intensity to minimise the presence of higher harmonics. The measurements were all carried out in transmission mode using optimised ionisation chambers as detectors. To minimise noise the counting time per data point was taken 1000 ms and at least three scans were recorded and averaged. All samples were recorded *ex situ* in He at 77 K. Energy calibration was performed by means of a V-foil (5 μm). The absolute value of the vanadium edge is 5465 eV.

The catalyst samples were pressed into self-supporting wafers and mounted in an EXAFS cell [27]. The thickness of the wafer was chosen in such a way as to give an absorbance (μx) of 2.5 for optimal signal-to-noise ratio. To prevent self-absorption by the catalysts the amount of sample was chosen such that a step in absorbance of 1.0 in the edge region ($\Delta\mu x = 1$) was obtained. If necessary, samples were diluted with boron nitride (BN). Standard procedures were used to extract the EXAFS data from the measured absorption spectrum. The background was subtracted using cubic spline routines [28]. Normalisation was done by dividing the data by the height of the absorption at 50 eV.

The ESR experiments were performed on an X-band Bruker ESP300 spectrometer equipped with an EN801 resonator (operating in TM110 cylindrical mode with unloaded $Q = 1000$). The microwave power was 1 mW, far below saturation levels for the supported V–P–O samples. The magnetic field was modulated with a frequency of 12.5 kHz and amplitude of 1 G. The sample temperature was adjusted in the range of 3.7–300 K with an Oxford ESR900 helium flow cryostat under control of an Oxford ITC503 temperature controller (temperature stability of 0.5 K).

3. Results and discussion

3.1. Catalyst performance

In figure 1 the conversion as a function of temperature of VPO/bulk, VPO/TiO_2 and VPO/SiO_2 is represented. It is obvious that VPO/TiO_2 is the most active catalyst, showing conversion at 473 K already. In general, our titania-supported catalysts are even more active at lower loadings [5]. Despite the lower amount of V–P–O present in the silica-supported catalyst, this sample is more active than the bulk catalyst. This difference can be explained by the higher specific surface area of the active component in the supported catalysts. The specific surface area (BET method) of the samples was determined to be 9 m^2/g for VPO/bulk, 54 m^2/g for VPO/SiO_2, and 44 m^2/g for VPO/TiO_2, respectively.

Both VPO/bulk and VPO/SiO_2 show about the same selectivity to maleic anhydride (figure 2). The optimum yield

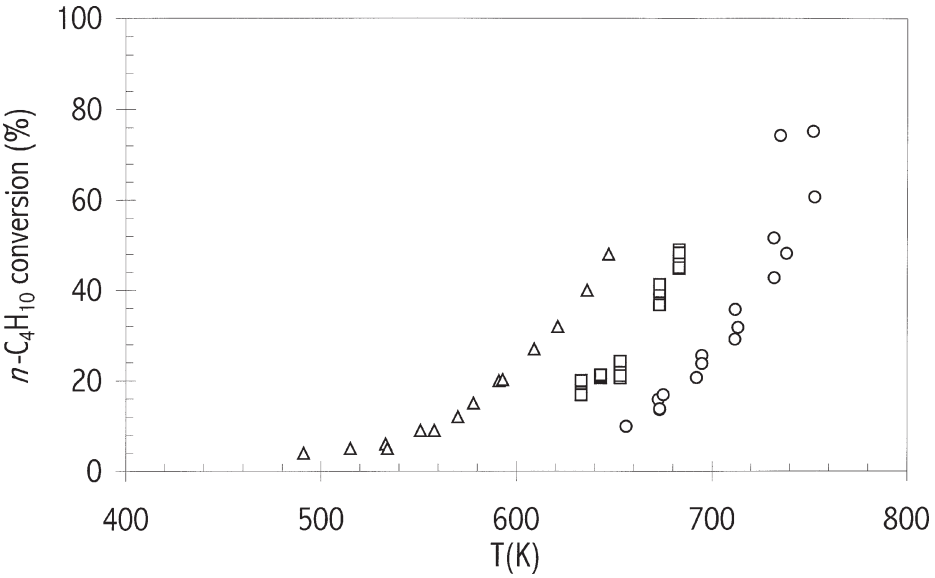

Figure 1. Conversion as a function of temperature for VPO/bulk (○), VPO/SiO_2 (□) and VPO/TiO_2 (△). Data were averaged over a period of 2 h and collected in an n-butane/oxygen/argon flow (1.5/20/78.5) of 50 ml/min at atmospheric pressure.

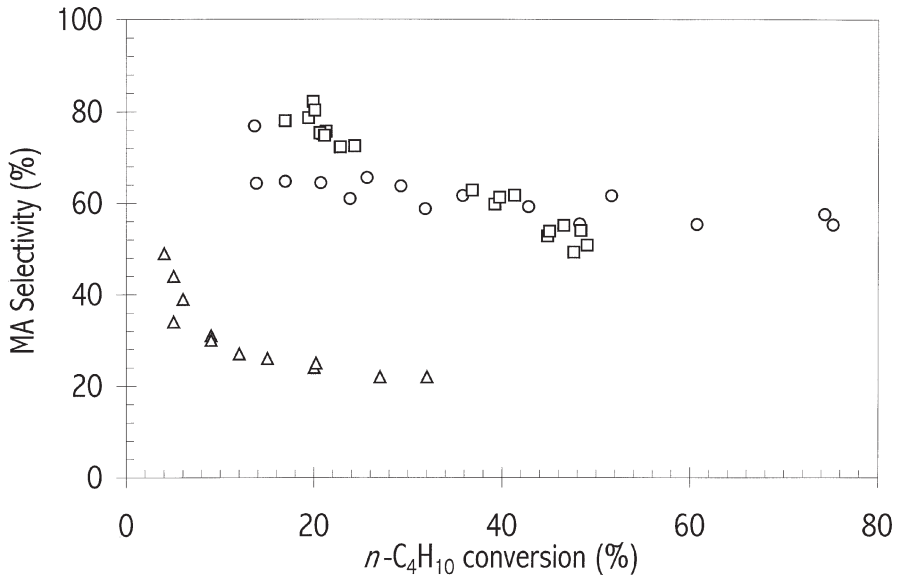

Figure 2. Selectivity as a function of conversion for VPO/bulk (○), VPO/SiO_2 (□) and VPO/TiO_2 (△).

for VPO/bulk and VPO/SiO_2 is 25–30% at a conversion of 50%. This might indicate that the nature of the active sites is the same. However, for VPO/SiO_2 the selectivity decreases much more when the conversion is raised. The selectivity of VPO/TiO_2 at low conversions is substantially below that of the other catalysts and only a yield of 6% is obtained at a conversion of 30%.

The differences in activity and selectivity between VPO/TiO_2 on the one hand and VPO/SiO_2 and VPO/bulk on the other hand, have been explained by the strong interaction between V–P–O and titania [5,7]. However, this does not explain the comparable yield to maleic anhydride for VPO/SiO_2 and VPO/bulk. Therefore we will focus on the structural characterisation of the various samples in the remaining part of this paper.

3.2. EXAFS

In figure 3 the k^2 Fourier transforms of VPO/bulk and VPO/SiO_2 are shown (0 Å $< R <$ 5 Å, no phase correction). It is obvious that the imaginary parts of the two Fourier transforms differ significantly around 1.5 Å. This is the range where the contributions of the first-shell oxygen atoms are located. Furthermore, an important extra contribution at $\pm$2 Å is present in the data of VPO/TiO_2. For the higher co-ordination shells the spectra of bulk and supported V–P–O differ considerably. A detailed description of the EXAFS data analysis of both bulk and of supported V–P–O catalysts will be published elsewhere [29].

Recently, Nguyen et al. have revealed the structure of crystalline vanadylpyrophosphate [18]. Our EXAFS data

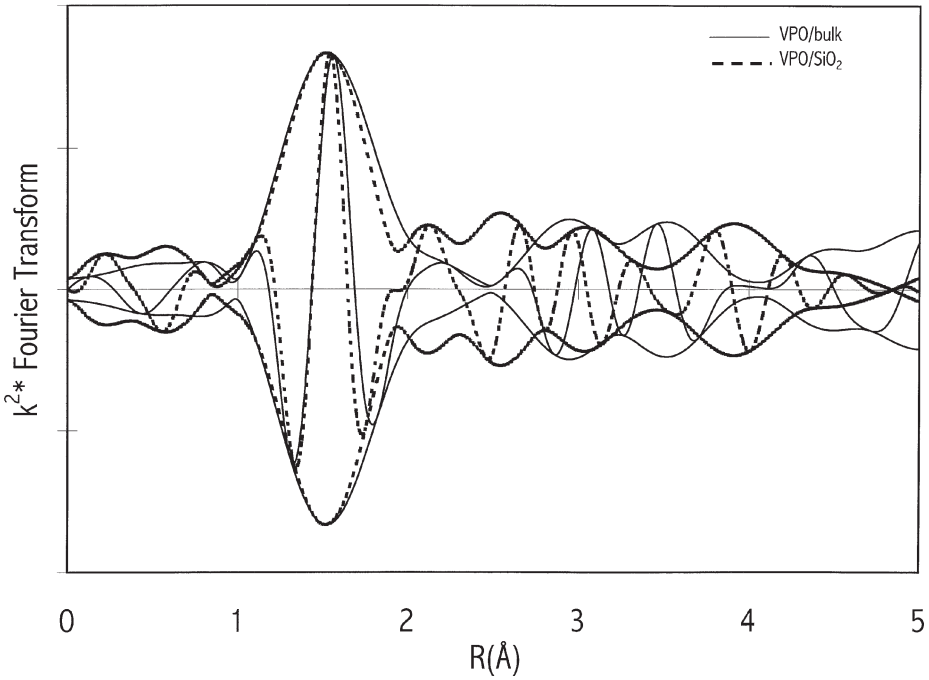

Figure 3. 0 Å $< R <$ 5 Å range of the k^2 Fourier transform of the EXAFS data of VPO/bulk (solid line) and VPO/SiO_2 (dotted line).

of VPO/bulk could be fitted up to a distance of 3.5 Å with the single-crystal X-ray data of Nguyen et al. [18]. Above this threshold too many contributions must be included in the calculations, which results in a low reliability of the final fit. The results of the EXAFS data analysis of our VPO/bulk have been published elsewhere [30].

Although an appreciable amount ($\pm$30%) of our bulk VPO sample consists of an amorphous V–P–O phase [31], the EXAFS spectrum is dominated by the structure of the ideally crystalline vanadylpyrophosphate phase. This makes techniques such as XRD and EXAFS inappropriate to study possible amorphous (surface) contributions in bulk V–P–O catalysts.

Figure 4 represents the k^2 Fourier transforms of the EXAFS data of both supported catalysts. For both supported samples, the magnitude of the Fourier transforms drops to zero at a distance of 5 Å from the vanadium atom. This is an indication that the samples do not exhibit long-range order, as is the case with VPO/bulk.

The spectra of the supported catalysts are markedly different from each other in both the first co-ordination shell and in the higher shells. It is important to note that the spectrum of VPO/TiO_2 also deviates from that of VPO/bulk. This means that the structure of both supported V–P–O catalysts differs from bulk crystalline $(VO)_2P_2O_7$.

As stated above, EXAFS is a technique that probes the local structure around the central vanadium atom up to a distance of about 4 Å. In principle, the EXAFS spectrum represents the superposition of both bulk and surface contributions. However, the EXAFS spectrum of VPO/SiO_2 is not suffering from interfering dominant bulk contributions and, hence, represents a clear picture of the local structure of the amorphous V–P–O phase at the surface.

Preliminary analysis of the EXAFS data indicates that VPO/TiO_2 consists of small particles, in which the V atoms are tetrahedrally co-ordinated by oxygen atoms, including V–O–Ti bridging oxygen atoms. The VPO/SiO_2 catalyst, on the other hand, consists of vanadyl groups in an octahedral environment. The XANES data of the samples (not shown) support this view.

It is important to note that with both supported V–P–O catalysts no V–V contributions were found in the EXAFS data up to a distance of 3.5 Å. To study the V–V interaction in the supported catalysts, we therefore have applied ESR spectroscopy.

3.3. ESR

ESR spectroscopy is a powerful technique to probe paramagnetic centres. The major part of V–P–O catalysts consists of V^{4+} phosphate (d^1) with electronic spin $S = 1/2$. When the supported catalysts contain only isolated vanadyl groups the ESR spectrum will appear as a characteristic octet of the hyperfine coupling with the ^{51}V nucleus ($I = 7/2$). In practice, the V hyperfine coupling is often unresolved in solid-state V–P–O samples [32]. This absence is attributed to strong exchange interactions between adjacent electron spins [33] which averages out the hyperfine interaction with the vanadium nucleus.

Figure 5 represents the ESR spectra of VPO/TiO_2 at different temperatures. At room temperature, the ESR spectra of the two supported catalysts correspond to the spectrum of VPO/bulk [31]. However, when the temperature is decreased, the spectrum of VPO/TiO_2 starts revealing the hyperfine coupling to the V nucleus. In contrast, for

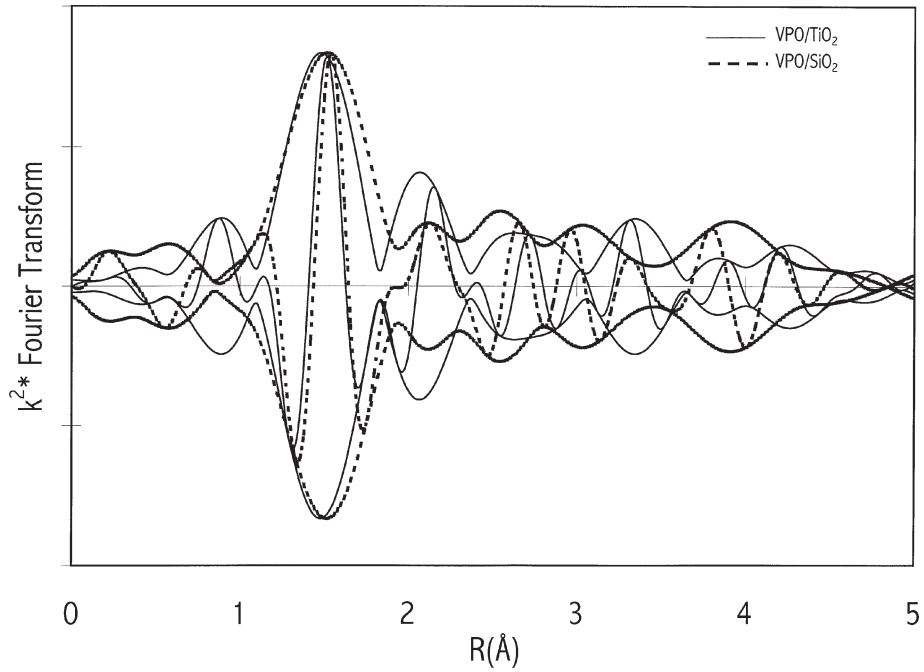

Figure 4. 0 Å $< R <$ 5 Å range of the k^2 Fourier transform of the EXAFS data of VPO/SiO_2 (dotted line) and VPO/TiO_2 (solid line).

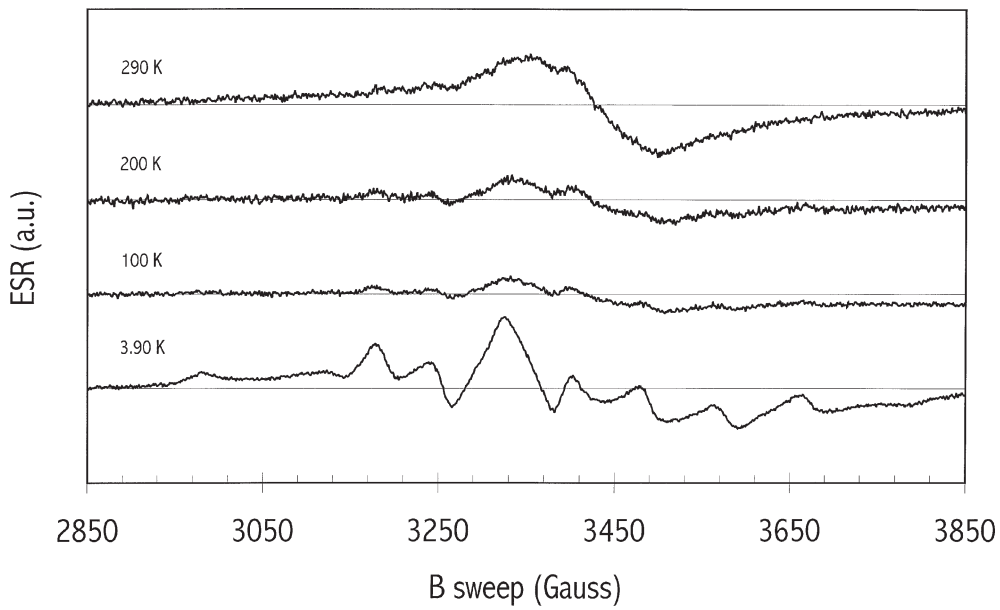

Figure 5. X-band ESR spectra of VPO/TiO_2 at different temperatures: 290, 200, 100 and 3.90 K. The magnetic field is centred at 3400 G, and swept over 1000 G. The spectra have been taken at a microwave frequency of 9.437 GHz.

VPO/SiO_2 the hyperfine coupling remains unresolved. This indicates that exchange interactions between neighbouring vanadyl groups dominate the hyperfine coupling down to very low temperatures. The strength of this interaction can be determined from the temperature dependence of the ESR intensity [31]. For bulk V–P–O we have previously found that its ESR spectrum contains three different contributions, i.e., strongly interacting vanadyl groups ($J/k = -65.7$ K), weakly interacting vanadyl groups ($J/k = -4.7$ K) and antiferromagnetic defects in a ratio of 10 : 7 : 2 [31].

In the paramagnetic regime ($T > T_{\text{Néel}}$), the ESR intensity, I, can be described by the Curie–Weiss equation for antiferromagnets:

$$I(T) \propto \frac{1}{T - \theta}. \tag{1}$$

The Curie–Weiss temperature, θ, can be extracted from a plot of the reciprocal of the total integrated ESR intensity of VPO/SiO_2 as a function of the temperature (figure 6).

For antiferromagnetically coupled pairs the Curie–Weiss temperature θ is related to the coupling parameter J via the

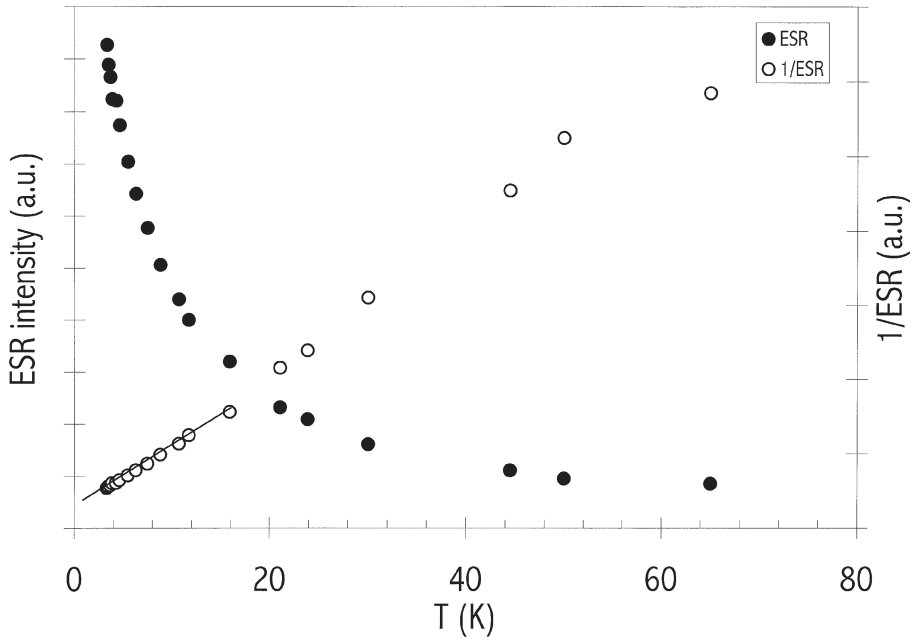

Figure 6. 1/ESR intensity as a function of temperature of VPO/SiO_2. The solid curve represents a fit of the data assuming Curie–Weiss behaviour. The Curie–Weiss temperature θ is extracted from the intersection and amounts to 2 ± 1 K.

relation $k\theta = -(3/2)J$. A linear dependence of the reciprocal ESR intensity and T indicates that the compound is exhibiting Curie–Weiss behaviour at low temperatures. The Curie–Weiss temperature is extrapolated to $\theta = 2 \pm 1$ K. This value is significantly lower than that measured with the VPO/bulk sample in which, in the amorphous part, antiferromagnetic coupling between vanadyl groups exists ($J/k = -4.7$ K, which corresponds to $\theta = 7.1$ K). However, this interaction is still strong enough to average out the hyperfine coupling in the ESR data down to the lowest temperatures accessible with our equipment (3.7 K).

The small value of the Curie–Weiss temperature in VPO/SiO_2 suggests that the average V–V distance in the amorphous V–P–O phase is considerably larger than 3.3 Å (the V–V distance in crystalline vanadylpyrophosphate). We then note that such a relatively large V–V distance cannot be observed with EXAFS.

4. Conclusions

In our study we have investigated V–P–O catalysts supported (on the surface) of silica and titania particles. Their catalytic performance was tested in the n-butane oxidation reaction to maleic anhydride, and the structure of the samples was characterised with EXAFS and ESR spectroscopy. Our results show considerable differences between VPO/TiO_2 and VPO/SiO_2 in catalytic performance, the local structure around vanadium (EXAFS) and spin exchange interactions between vanadium atoms (ESR). The combination of characterisation methods has revealed that the structure of the supported V–P–O phase does not match crystalline vanadylpyrophosphate.

There are three strong indications that the amorphous V–P–O phase in VPO/SiO_2 resembles the real active phase of bulk V–P–O catalysts: (i) catalytic selectivity, (ii) catalytic yield, (iii) EXAFS.

We therefore propose that the oxidation of n-butane to maleic anhydride takes place over an amorphous surface V–P–O phase. This finding has high relevance for our understanding of the catalytic activity of bulk crystalline V–P–O catalysts as well.

Therefore, it will be interesting to study the structure of the VPO/SiO_2 catalyst in more detail, as it may serve as a model for the amorphous component in bulk V–P–O catalysts. A detailed analysis of the EXAFS data of this sample as well as application of other characterisation techniques can give more insight in the nature of the real active site of the maleic anhydride catalyst.

References

[1] B.K. Hodnett, Catal. Rev. Sci. Eng. 27 (1985) 373.
[2] G. Centi, F. Trifirò, J.R. Ebner and V.M. Franchetti, Chem. Rev. 88 (1988) 55.
[3] G. Centi, Catal. Today 16 (1993) 5.
[4] M. Abon and J.C. Volta, Appl. Catal. A 157 (1997) 173.
[5] R.A. Overbeek, P.A. Warringa, M.J.D. Crombag, L.M. Visser, A.J. van Dillen and J.W. Geus, Appl. Catal. A 135 (1996) 209.
[6] R.A. Overbeek, A.R.C.J. Pekelharing, A.J. van Dillen and J.W. Geus, Appl. Catal. A 135 (1996) 231.
[7] M. Ruitenbeek, R.A. Overbeek, A.J. van Dillen, D.C Koningsberger and J.W. Geus, Recl. Trav. Chim. Pays-Bas 115 (1996) 519.
[8] V.A. Zazhigalov, Yu.P. Zaitsev, V.M. Belousov, B. Parlitz, W. Hanke and G. Ohlman, React. Kinet. Catal. Lett. 32 (1986) 209.
[9] K.E. Birkeland, S.M. Babitz, G.K. Bethke, H.H. Kung, G.W. Coulston and S.R. Bare, J. Phys. Chem. B 101 (1997) 6895.
[10] J.M.C. Bueno, G.K. Bethke, M.C. Kung and H.H. Kung, Catal. Today 43 (1998) 101.

[11] M. Martinez-Lara, L. Moreno-Real, R. Pozas-Tormo, A. Jiminez-Lopez, S. Bruque, P. Ruiz and G. Poncelet, Canad. J. Chem. 70 (1992) 5.
[12] M. Nakamura, K. Kawai and Y. Fujiwara, J. Catal. 34 (1974) 345.
[13] N.T. Do and M. Baerns, Appl. Catal. 45 (1988) 1.
[14] A. Ramstetter and M. Bearns, J. Catal 109 (1988) 303.
[15] P.S. Kuo and B.L. Yang, J. Catal. 117 (1989) 301.
[16] E. Bordes, Catal. Today 1 (1987) 499.
[17] G.J. Hutchings, A. Desmartin-Chomel, R. Olier and J.C. Volta, Nature 368 (1994) 41.
[18] P.T. Nguyen, R.D. Hoffman and A.W. Sleight, Mater. Res. Bull. 30 (1995) 1055.
[19] P.A. Agaskar, L. DeCaul and R.K. Graselli, Catal. Lett. 23 (1994) 339.
[20] B. Schiott and K.A. Jorgensen, Catal. Today 16 (1993) 79.
[21] M.T. Sananes, A. Tuel and J.C. Volta, J. Catal. 145 (1994) 251.
[22] N. Harrouch Batis, H. Batis, A. Ghorbel, J.C. Vedrine and J.C. Volta, J. Catal. 128 (1991) 248.
[23] G. Bergeret, M. David, J.P. Broyer, J.C. Volta and G. Hecquet, Catal. Today 1 (1987) 37.
[24] K. Katsumoto and D.M. Marquis, US Patent 4,132,670 (1970).
[25] R.A. Overbeek, M. Versluijs-Helder, P.A. Waaringa, E.J. Bosma and J.W. Geus, Stud. Surf. Sci. Catal. 82 (1994) 183.
[26] R.A. Overbeek, E.J. Bosma, D.W.H. de Blauw, A.J. van Dillen, H.G. Bruil and J.W. Geus, Appl. Catal. 163 (1997) 129.
[27] M. Vaarkamp, B.L. Mojet, J.T. Miller and D.C. Koningsberger, J. Phys. Chem. 99 (1995) 16067.
[28] J.B.A.D. van Zon, D.C. Koningsberger, H.F.J. van Blik and D.E.J. Sayers, J. Chem. Phys. 82 (1985) 5742.
[29] M. Ruitenbeek, A.J. van Dillen, J.W. Geus and D.C. Koningsberger, in preparation.
[30] M. Ruitenbeek, R.A. Overbeek, D.C. Koningsberger and J.W. Geus, in: *Catalytic Activation and Functionalisation of Light Alkanes*, eds. E.G. Derouane et al. (Kluwer, Dordrecht, 1998) p. 423.
[31] M. Ruitenbeek, A. Barbon, E.E. van Faassen and J.W. Geus, Catal. Lett. 54 (1998) 101.
[32] Y. Zhang-Lin, M. Forissier, J.C. Vedrine and J.C. Volta, J. Catal. 145 (1994) 267.
[33] A. Bencini and D. Gatteschi, *EPR of Exchange Coupled Systems* (Springer, Berlin, 1990).